ISSN 0036-0236, Russian Journal of Inorganic Chemistry, 2011, Vol. 56, No. 5, pp. 792–797. © Pleiades Publishing, Ltd., 2011.
Original Russian Text © O.V. Andreev, A.V. Ruseikina, L.A. Solov'ev, 2011, published in Zhurnal Neorganicheskoi Khimii, 2011, Vol. 56, No. 5, pp. 843–848.

PHYSICOCHEMICAL ANALYSIS OF INORGANIC SYSTEMS

Phase Diagrams of Sections in the $EuS–Cu_2S–Nd_2S_3$ System

O. V. Andreev[a], A. V. Ruseikina[a], and L. A. Solov'ev[b]

[a] *Tyumen State University, ul. Semakova 10, Tyumen, 625003 Russia*

[b] *Institute of Chemistry and Chemical Engineering, ul. Karla Marksa 42, Krasnoyarsk, 660049 Russia*

Received July 7, 2010

Abstract—Phase equilibria in the $EuS–Cu_2S–Nd_2S_3$ system were studied in an isothermal (970 K) section and $NdCuS_2–EuS$ and $Cu_2S–EuNdCuS_3$ polythermal sections. The complex sulfide $EuNdCuS_3$ has an orthorhombic crystal lattice (space group *Pnma*; $a = 1.10438(2)$ nm, $b = 0.40660(1)$ nm, $c = 1.14149(4)$ nm), is isostructural to $BaLaCuS_3$, and melts incongruently at 1470 K: $EuNdCuS_3$ (0.50 EuS; 0.50 $NdCuS_2$) $\rightleftharpoons$ 0.18 EuS ss (0.88 EuS; 0.12 $NdCuS_2$) + 0.82 L (0.415 EuS; 0.585 $NdCuS_2$); $\Delta H = 17.8$ kJ/mol. Within the range 0.5 mol % EuS, $EuNdCuS_3$-based solid solutions were not found. At 970 K, the tie lines pass from the compound $EuNdCuS_3$ to Cu_2S, EuS, $NdCuS_2$, and $EuNd_2S_4$ phases and lie between the $NdCuS_2$ phase and solid solutions (ss) of γ-Nd_2S_3 with $EuNd_2S_4$. Eutectics are formed between the compounds $NdCuS_2$ and $EuNdCuS_3$ at 32.0 mol % EuS $T = 1318$ K and between the compounds Cu_2S and $EuNdCuS_3$ at 20.5 mol % $EuNdCuS_3$ and $T = 1142$ K. Five main subordinate triangles were identified in the system.

DOI: 10.1134/S0036023611040024

We failed to find any data on phase equilibria in the $EuS–Cu_2S–Nd_2S_3$ ternary system. The $Cu_2S–Nd_2S_3$ system forms a complex sulfide $NdCuS_2$, which melts incongruently at 1465 K [1]. A eutectic between Cu_2S and $NdCuS_2$ phases is formed at 17 mol % Nd_2S_3 and $T = 1267$ K. The $Nd_2S_3–EuS$ system forms a complex compound $EuNd_2S_4$ [2, 3], which melts incongruently at 2430 K [4]. A continuous solid solution having a Th_3P_4 type structure is formed between γ-Nd_2S_3 and $EuNd_2S_4$. A eutectic between the phases $EuNd_2S_4$ and EuS is formed at 66.5 mol % EuS and $T = 2290$ K. No new compounds were found in the $Cu_2S–EuS$ system. The composition of a eutectic is 24.5 mol % EuS and $T = 1069$ K [5].

A study of phase equilibria in the $EuS–Cu_2S–Nd_2S_3$ system is topical because a combination of sulfides of *d* and 4*f* elements gives new compounds and the information contained in the phase diagrams serves as the basis for determining their synthesis conditions.

The purpose of this work was to investigate phase equilibria in the $EuS–Cu_2S–Nd_2S_3$ system in an isothermal (970 K) section and polythermal sections and determine the composition and structural characteristics of a new complex sulfide.

EXPERIMENTAL

The compound Cu_2S was produced from the constituent elements (copper of 11-4 high-purity grade and sulfur of 15-3 high-purity grade) in sealed evacuated double-walled quartz ampoules. The sulfides EuS and Nd_2S_3 were synthesized from oxides of the grades "EvO-Zh" and "NO-Zh", respectively, in a flow of H_2S and CS_2 at 1300 K [6].

In the $EuS–Cu_2S–Nd_2S_3$ system, 70 samples the compositions of which fell inside the composition triangle were synthesized from the initial sulfides Cu_2S, EuS, and Nd_2S_3. Mixtures of oxides were alloyed according to published procedures [6]. The samples were annealed at 970 K for 3000 h in sealed evacuated quartz ampoules. Then, the samples were kept for 0.5 h at 1770 K in an open reactor while inductively heating a graphite crucible and, after that, annealed for 3 h at 1450 K in evacuated double-walled quartz ampoules in an electrically heated furnace. The results of microstructural analysis, X-ray powder diffraction, and differential scanning calorimetry of the samples during annealing suggest that they have reached equilibrium.

Thermal analysis was performed on a Setsys Evolution 1750 (TGA-DSC 1600) thermal analysis setup according to previously developed procedures using the SETSOFT 2000 program package [7]. Overlapping peaks were resolved using the Thermogram Analyzer program. Visual polythermal analysis was carried out with accuracy precision of 1%. Microstructural analysis was made with a METAM RV-22 microscope. The hardness was measured with a PMT-3M meter by the Vickers method with a precision of 5–7%. The graphical representation was made using the Edstate 2D and Edstate 3D software. X-ray powder diffraction data were obtained on a Dron-7 diffractometer and a PANalytical X'Pert PRO diffractometer equipped with a PIXcel detector (CoK_α radiation, $10° \le 2\theta \le 120°$). The $EuNdCuS_3$ lattice parameters were

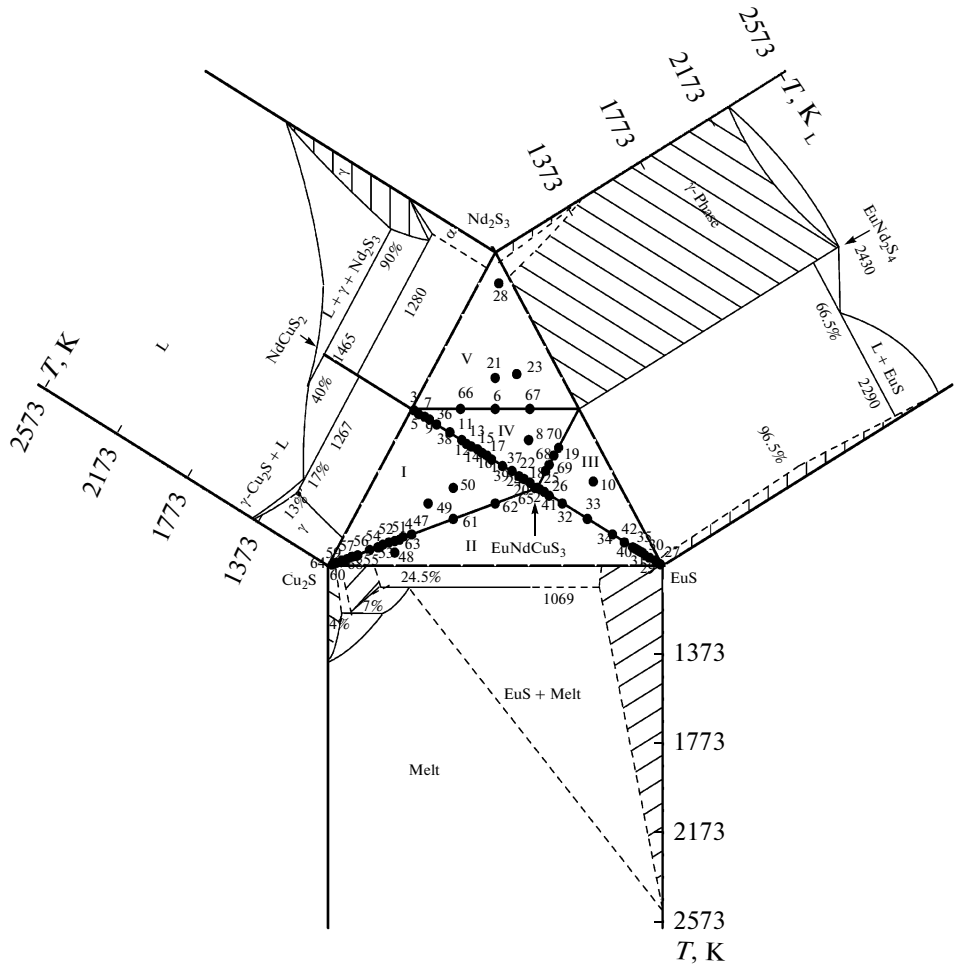

Fig. 1. Positions of tie lines in the EuS–Cu_2S–Nd_2S_3 system at 970 K. Dots represent studied samples; the Roman numerals, main subordinate triangles.

determined using the ITO program [8]. The $EuNdCuS_3$ crystal structure was refined by the derivative difference minimization method [9] with the confidence factors R-DDM = 8.49% and R_B = 4.6%. Data on the isostructural compound $BaLaCuS_3$ were used as the initial model [10, 11].

RESULTS AND DISCUSSION

In the EuS–Cu_2S–Nd_2S_3 system at the EuS to Cu_2S to Nd_2S_3 ratio of 2 : 1 : 1, a complex sulfide $EuNdCuS_3$ forms. The compound is isostructural to $BaLaCuS_3$ and has an orthorhombic crystal lattice (space group *Pnma*) with the unit cell parameters a = 1.10438(2) nm, b = 0.40660(1) nm, and c = 1.14149(4) nm. Multistructural analysis and X-ray powder diffraction showed that $EuNdCuS_3$ is in equilibrium with Cu_2S, EuS, $NdCuS_2$, and $EuNd_2S_4$, which allows one to determine the positions of tie lines at 970 K (Fig. 1). There is also equilibrium between the $NdCuS_2$ phase and solid solutions of γ-Nd_2S_3 with $EuNd_2S_4$ having a Th_3P_4 type structure. Five main subordinate triangles were identified in the system (Fig. 1): $NdCuS_2$–$EuNdCuS_3$–Cu_2S (**I**), Cu_2S–$EuNdCuS_3$–EuS (**II**), EuS–$EuNdCuS_3$–$EuNd_2S_4$ (**III**), $NdCuS_2$–$EuNdCuS_3$–$EuNd_2S_4$ (**IV**), and $NdCuS_2$–Nd_2S_3–$EuNd_2S_4$ (**V**).

The compound $EuNdCuS_3$ is in equilibrium with $NdCuS_2$ and EuS phases. The phase diagram of the $NdCuS_2$–EuS system has been constructed for the first time (Fig. 2a).

Crystals of the complex sulfide $EuNdCuS_3$ ($1NdCuS_2$: 1EuS) in the microstructural analysis are gray-brown, and H = 2320 MPa (P = 0.02 kg). The compound melts incongruently. The average onset temperature of the phase-transformation peak is 1470 K. The heat of melting of the compound is 17.8 kJ/mol. The incongruent melting tie line touches the EuS-based solid solution and the liquid, which enables one to write a thermochemical equation of phase transformation (table).

No homogeneity regions based on the compounds $NdCuS_2$ and $EuNdCuS_3$ were found. According to X-ray powder diffraction and microstructural analysis,

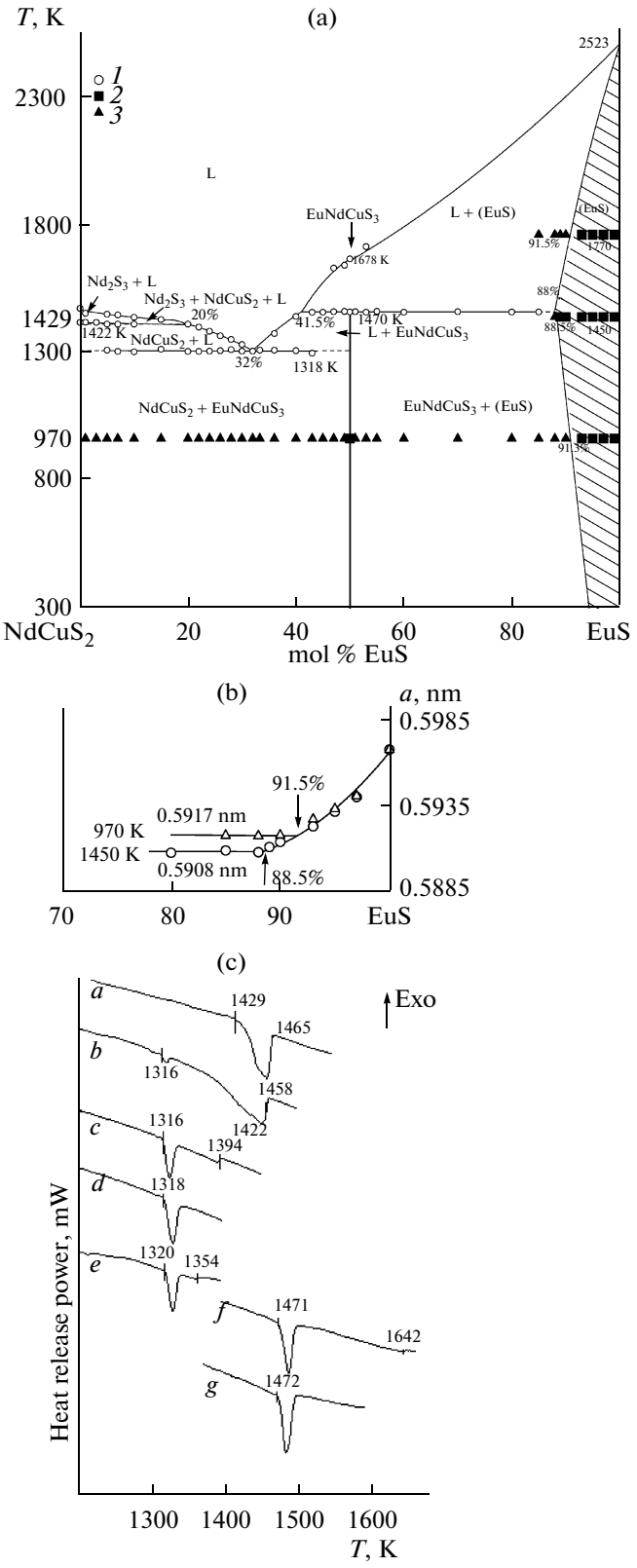

Fig. 2. (a) Phase diagram of the $NdCuS_2$–EuS system: (*1*) DSC data; the states of samples according to X-ray powder diffraction and microstructural analysis: (*2*) single-phase and (*3*) two-phase. (b) Variations in the parameters of the NaCl-type unit cell in the EuS ss region. (c) DTA events for samples containing (*a*) 1.0, (*b*) 7.0, (*c*) 24.0, (*d*) 26.0, (*e*) 33.3, (*f*) 47.0, and (*g*) 55.0 mol % EuS.

Table

Type of phase transformation	Incongruent melting of compound		Phase transformation equation	ΔH_m, J/g, kJ/mol
	composition	T, K		
Incongruent melting of compound	$EuNdCuS_3$ ($1NdCuS_2$: 1EuS)	1470	$EuNdCuS_{3\,(solid)}$ (0.50 EuS; 0.50 $NdCuS_2$) $\rightleftharpoons$ 0.18 ss EuS (0.88 EuS; 0.12 $NdCuS_2$) + 0.82 L (0.415 EuS; 0.585 $NdCuS_2$)	39 17.8
Melting of eutectic in the $NdCuS_2$–EuS system	32.0 mol % EuS	1318	0.36 $NdCuS_{2(solid)}$ + 0.64 $EuNdCuS_3$ (0.50 EuS; 0.50 $NdCuS_2$) $\rightleftharpoons$ L (0.32 EuS; 0.68 $NdCuS_2$)	22
Incongruent melting of compound	$NdCuS_2$ ($1Cu_2S$: $1Nd_2S_3$)	1429	$NdCuS_{2\,(solid)}$ (0.50 Nd_2S_3; 0.50 Cu_2S) $\rightleftharpoons$ 0.80 L (0.40 Nd_2S_3; 0.60 Cu_2S) + 0.20 ss γ-Nd_2S_3 (0.90 Nd_2S_3; 0.10 Cu_2S)	51 13.9
Melting of eutectic in the Cu_2S–$EuNdCuS_3$ system	20.5 mol % $EuNdCuS_3$	1142	0.87 ss Cu_2S (0.085 $EuNdCuS_3$; 0.915 Cu_2S) + 0.13 $EuNdCuS_{3\,(solid)}$ $\rightleftharpoons$ L (0.205 $EuNdCuS_3$; 0.795 Cu_2S)	12

samples containing 1.0, 3.0, 47.0, 49.0, 51.0, and 53.0 mol % EuS comprise two phases; the amount of a second phase corresponds to the position of the sample in the diagram. The changes in the unit cell parameters of two-phase samples annealed at 970 K relative to homogeneous samples fall within the measurement errors.

A temperature-dependent region of EuS-based solid solution is formed (Fig. 2b). Within the homogeneity range, the parameter a decreases from 0.5967 to 0.5908 nm at 1450 K and to 0.5917 nm at 970 K, which agrees with the value of the reduced cation radius: $r(Cu^+, Nd^{3+}) = (0.0600 + 0.0.1109)/2 = 0.0855$ nm [12]. The negative deviation from Vegard's rule suggests that the interaction between the components of the EuS matrix is weaker than the interaction with the doping components. Using the dependence of the parameter a on the composition and the emergence of a second phase in the samples, we determined the positions of solidus points (1770 K, 91.5 mol % EuS) and solvus points (1450 K, 88.5 mol % EuS and 970 K, 91.5 mol % EuS).

The equation of the reaction of incongruent decomposition of $NdCuS_2$ was composed based on the phase diagram of the Cu_2S–Nd_2S_3 system [1]. The heat of incongruent melting of $NdCuS_2$ was found to be 13.9 kJ/mol (table). The heat of melting of Cu_2S is 11.296 ± 0.209 kJ/mol [13]. The enthalpy of melting of $NdS_{1.37}$ is 45.0 kJ/mol [14]. The heat of melting of γ-Nd_2S_3 might be expected to be of the same order. The similarity of the heats of melting of $NdCuS_2$ and Cu_2S agrees with the formation of 0.20 moles of crystalline solid solution of γ-Nd_2S_3 in the course of the incongruent melting.

Within the range 0–50 mol % EuS, a eutectic between the phases $NdCuS_2$ and $EuNdCuS_3$ is formed. The eutectic temperature was found by averaging the temperatures for 15 samples of various compositions and was taken to be 1318 K (Fig. 2c). The composition of the eutectic according to the microstructural analysis data and the data obtained by constructing the Tammann triangle is 32 mol % EuS. According to DSC data, the heat is 22 J/g (table). In the $NdCuS_2$–eutectic region, the eutectic mixture on polished sections of samples is represented by alternating oval crystals of sulfide phases 10–20 μm in size. In the eutectic–$EuNdCuS_3$ region, eutectic grains of conjugate phases are also oval, but their colors are similar and interfaces are diffuse even on etching.

The liquidus line in the $NdCuS_2$–eutectic region consists of two branches which were constructed by fitting the DSC data by second-order polynomials. The branch of the liquidus line that corresponds to the primary crystallization of γ-Nd_2S_3 solid solution grains 3 touches the $NdCuS_2$ incongruent melting surface. The coordinates of the point of touch are ~20 mol % EuS and $T = 1422$ K.

Between the Nd_2S_3 + liquid and $NdCuS_2$ + liquid fields, there is is the Nd_2S_3 + $NdCuS_2$ + liquid field (outlined by dashed line). We constructed the side of the Tammann triangle that represents the dependence of the area of the $NdCuS_2$ incongruent melting peak on the molar composition for samples containing 0.0–0.15 mol % EuS. At 0.0 mol % EuS, the peak area is maximal. The obtained heat value (13.9 kJ/mol) coincides with the heat of incongruent melting of $NdCuS_2$ (table).

Within the range 50–100 mol % EuS at temperatures below the $EuNdCuS_3$ incongruent melting temperature, $EuNdCuS_3$ and a EuS-based solid solution are in equilibrium. The reflections of these phases were only detected in the X-ray diffraction patters of the samples annealed at 970 K. On polished sections, there are brown oval EuS grains ($H = 1300$ MPa) 5×10 to 50×70 μm in size, located inside the field of the $EuNdCuS_3$ phase ($H = 2320$ MPa). The microstructure of the samples cooled from melt is formed by primary oval EuS grains located inside the field of the $EuNdCuS_3$ phase, and some areas include regions of a eutectic between the $EuNdCuS_3$ and $NdCuS_2$ phases.

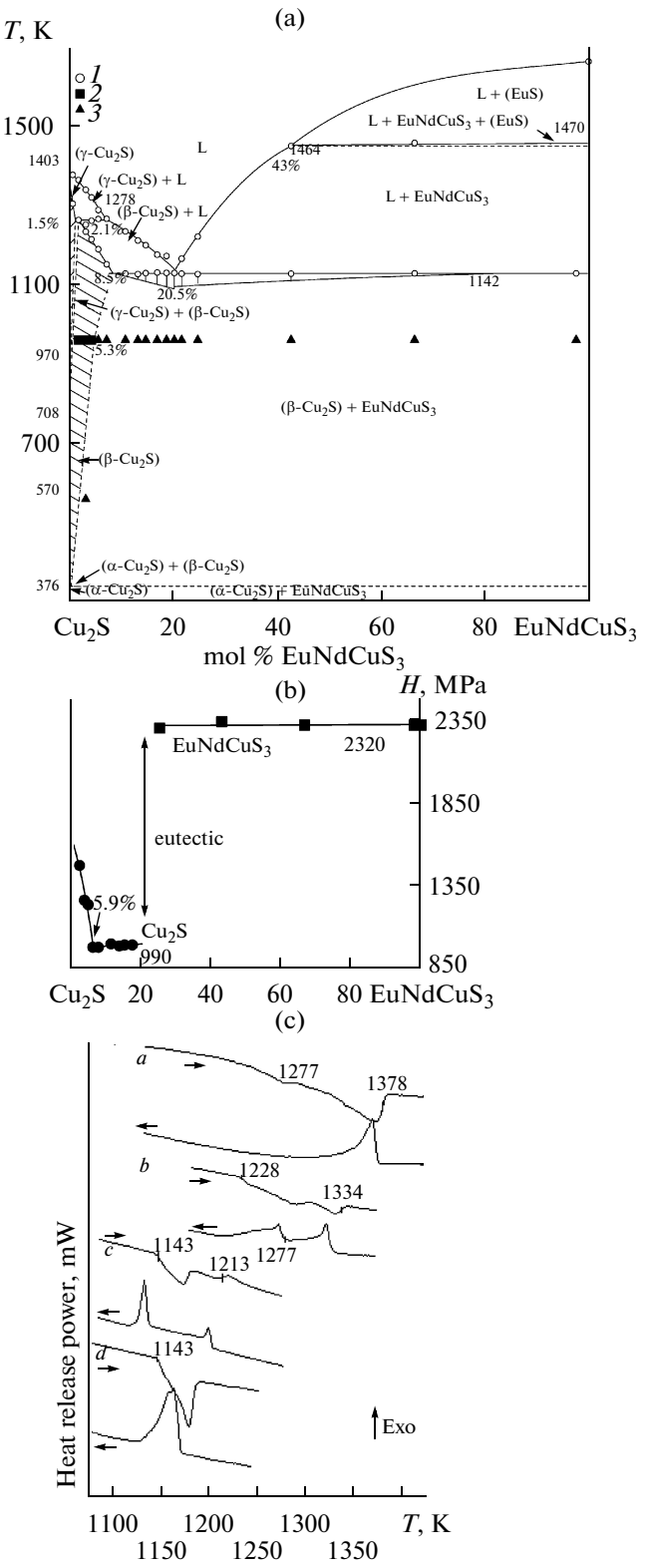

Fig. 3. (a) Phase diagram of the Cu_2S–$EuNdCuS_3$ system: (*1*) DSC data; the states of samples according to X-ray powder diffraction and microstructural analysis: (*2*) single-phase and (*3*) two-phase. (b) Microhardness versus composition diagram. (c) DTA events for samples containing (*a*) 2.1, (*b*) 4.6, (*c*) 15.0, and (*d*) 20.5 mol % $EuNdCuS_3$.

The microstructural analysis of quenched and annealed samples confirmed the incongruent melting of $EuNdCuS_3$.

The thermoanalytical curves of annealed samples containing 43.0–85.0 mol % EuS have a peak of $EuNdCuS_3$ incongruent melting (Fig. 2c). The average temperature is 1470 ± 2 K, which coincides with the average incongruent melting temperature of $EuNdCuS_3$. Differential scanning calorimetry gave the melt-transition temperatures for samples containing up to 55.0 mol % EuS. The thermogravimetric data at $T > 1740$ K show weight loss caused probably by thermal dissociation. The branch of the liquidus line was constructed using the data on the EuS melting point (2523 K [15]).

The phase diagram of the Cu_2S–$EuNdCuS_3$ system is of the eutectic type and is characterized by the presence of an unclosed region of solid solution based on β-Cu_2S and α-Cu_2S and a closed region of solid solution based on γ-Cu_2S (Fig. 3a).

The region of β-Cu_2S based solid solution has a polygonal shape, the solubility in the solid state is temperature dependent, and the solid solution decomposes incongruently. The onset temperatures of heat absorption were determined from the differential thermal analysis curves for samples containing 2.1–7.5 mol % $EuNdCuS_3$ (Fig. 3c). The solidus temperatures were fitted by a second-order polynomial. At the eutectic temperature 1142 K, the solidus is extrapolated to the composition 8.5 mol % $EuNdCuS_3$. The peak temperature of the decomposition peak for the β-Cu_2S-based solid solution was detected to be at 1278 K. The peritectoid-point composition (2.1 mol % $EuNdCuS_3$) was determined by constructing the Tammann triangle and extrapolating the solidus line. The horizontal line of incongruent decomposition of the β-Cu_2S-based solid solution intersects the liquidus line at 7.5 mol % $EuNdCuS_3$. In a sample containing 1 mol % $EuNdCuS_3$, the onset temperature of heat absorption is 1318 K and corresponds to the solidus of γ-Cu_2S-based solid solution. The composition at the point of intersection of the horizontal line and the region of γ-Cu_2S-based solid solution was taken to be 1.5 mol % $EuNdCuS_3$. We composed the equation of the incongruent decomposition of β-Cu_2S-based solid solution: β-Cu_2S ss (0.021 $EuNdCuS_3$; 0.979 Cu_2S) $\rightleftharpoons$ 0.9 γ-Cu_2S ss (0.015 $EuNdCuS_3$; 0.985 Cu_2S) + 0.1 L (0.075 $EuNdCuS_3$; 0.925 Cu_2S).

The β- and γ high-temperature phases of Cu_2S are not fixed by quenching [1]. Within the solid-solution region, the phase-transformation kinetics was observed. For samples annealed and quenched from 970 K, the reflections of the following phases were detected: α-Cu_2S ss (1.0 mol % $EuNdCuS_3$); α-Cu_2S ss and β-Cu_2S ss (2.1, 3.5, and 4.6 mol %) with continuously increasing β-Cu_2S content; β-Cu_2S ss (5.9 mol %); and β-Cu_2S ss and $EuNdCuS_3$ (7.5–97.6 mol %). The

parameters of the hexagonal unit cell of β-Cu_2S are a = 0.396 nm, c = 0.678 nm [16]. Within the solid-solution region, there is scatter of experimental values for the Cu_2S unit cell parameters as functions of composition. For 5.9 mol % $EuNdCuS_3$, the unit cell parameters are a = 0.395 nm, c = 0.674 nm.

According to microstructural analysis, samples containing up to 4.6 mol % $EuNdCuS_3$ are homogeneous. In samples containing 5.9 and 7.5 mol % $EuNdCuS_3$, the field of the Cu_2S phase is pierced throughout its volume by needle-shaped intrusions of 10–100-μm-long, 2–5-μm-wide gray-brown crystals of the conjugate phase $EuNdCuS_3$; there is no eutectic. The shape, size, and distribution of grains of the $EuNdCuS_3$ phase suggest solid-phase decomposition of the primary β-Cu_2S solid solution. In an initially homogeneous sample (5.9 mol % $EuNdCuS_3$) annealed at 970 K, needle-shaped crystals of the $EuNdCuS_3$ phase appear, which is indicative of the temperature dependence of solubility in solid β-Cu_2S.

Within the homogeneity region, the Cu_2S microhardness decreases from 1470 to 990 MPa (Fig. 3b), which is indicative of incorporation of ions having a larger radius ($r$$Eu^{2+}$(VII) = 0.12 nm [12]).

A eutectic is formed between β-Cu_2S ss and $EuNdCuS_3$ phases. The peak of melting of the eutectic has a pronounced linear portion and is detected at an average temperature of 1142 K. As the eutectic composition is approached, the sizes of Cu_2S primary yellow grains and $EuNdCuS_3$ gray-brown grains systematically decrease from 200 × 30 to 60 × 20 μm (H = 990 MPa) and from 900 × 50 to 60 × 20 μm (H = 2320 MPa). Crystals of the phases in the eutectic are 10 × 20 μm in size. According to the Tammann triangle construction and microstructural analysis, the eutectic composition was taken to be 20.5 mol % $EuNdCuS_3$, with the heat of melting being 12 J/g. A phase transformation equation was composed (table).

Between the EuS + L and $EuNdCuS_3$ + L fields in the system under investigation, there should be a EuS + $EuNdCuS_3$ + L field (outlined by dashed line). DSC detected a weak decrease in the $EuNdCuS_3$ melting point from 1470 to 1464 K. The coordinates of the point of intersection of the liquidus line and the line of phase decomposition of the compound $EuNdCuS_3$ are 43.0 mol % $EuNdCuS_3$ and T = 1464 K.

In the $EuNdCuS_3$–$EuNd_2S_4$ system, $EuNdCuS_3$ and $EuNd_2S_4$ phases are in equilibrium at the isothermal-section temperature of 970 K. No change was detected in the unit cell parameter within the two-phase region relative to the individual compounds, which is indicative of the absence of reciprocal solid solutions. A eutectic is formed between the phases, and the melting peak was detected at 1467 K and a composition of ~(30.0 ± 3.0) mol % $EuNd_2S_4$.

In the $NdCuS_2$–$EuNd_2S_4$ system at the isothermal-section temperature, the $NdCuS_2$ phase and the γ phase are in equilibrium. X-ray powder diffraction pattern showed no noticeable regions of homogeneity. No changes were detected in the unit cell parameter of the conjugate phases in the two-phase region. On polished sections, there are grains of the $NdCuS_2$ phase (H = 3350 MPa), located inside the fields of γ phase crystals (H = 5520 MPa).

ACKNOWLEDGMENTS

This work was supported by the Federal Target Program "Research and Research-Teaching Staff in Innovative Russia" for 2009–2013 (state contract nos. 6K/143-09 (P646) and NK-409/5 (P2263)).

REFERENCES

1. O. V. Andreev, Extended Abstract of Doctoral Dissertation in Chemistry (Tyumen, 1999).
2. M. Sato, G. Y. Adachi, and J. Shiokawa, J. Solid State Chem. **31**, 337 (1980).
3. A. A. Eliseev, O. A. Sadovskaya, and G. M. Kuzmicheva, J. Inorg. Mater. (Engl. Transl.) **18**, 1435 (1982).
4. A. V. Ruseikina and O. V. Andreev, *Proceedings of the All-Russia Scientific Conference "Solid-State Chemistry and Functional Materials"* (Yekaterinburg, 2008), p. 304 [in Russian].
5. A. V. Rusejkina, O. V. Andreev, and N. A. Khritokhin, *Proceedings of XVII International Conference on Chemical Thermodynamics in Russia* (Kazan, 2009), Vol. 2, p. 306 [in Russian].
6. V. G. Bamburov and O. V. Andreev, Zh. Neorg. Khim. **47** (4), 676 (2002) [Russ. J. Inorg. Chem. **47** (4), 598 (2002)].
7. A. V. Ruseikina, A. S. Zalineeva, and O. V. Andreev, in *Physicochemical Analysis of Natural and Engineering Systems: Collected Works* (Tyumen, 2008), p. 159 [in Russian].
8. J. W. Visser, J. Appl. Crystallogr. **2**, 89 (1996).
9. L. A. Solovyov, J. Appl. Crystallogr. **37**, C. 743 (2004).
10. A. E. Christuk, P. Wu, and J. A. Ibers, J. Solid State Chem. **110**, 330 (1994).
11. P. Wu, A. E. Christuk, and J. A. Ibers, J. Solid State Chem. **110**, 337 (1994).
12. R. D. Shannon, Acta Crystallogr. **32**, 751 (1976).
13. Database "The Thermal Constants of materials" http://www.chem.msu.su/cgi_bin/tkv.pl.
14. L. G. Gorbunova, Extended Abstract of Candidate's Dissertation in Chemistry (Novosibirsk, 1990).
15. *Phase Diagrams for Binary Metallic Systems: A Handbook*, Ed. by N. P. Lyakishev (Mashinostroenie, Moscow, 1996), Vol. 1, p. 475 [in Russian].
16. O. Andreev, Russ. J. Inorg. Chem. **34**, 909 (1989).